a 10-ms pulse. This could perhaps be understood if the bubbles generated by a 2-ms pulse are much smaller than those resulting from a 10-ms pulse. They dissolve more rapidly because of their greater internal pressure $2\sigma/r$ (σ, surface energy; r, radius).

The new phenomenon is discussed now which was observed in the experiments of Figure 7a when the on/off ratio was 1:500. Under these circumstances the pulses after the initial one became rapidly less efficient. The effect can be understood if one postulates that the fresh solution contained "natural" nuclei, X_n, which are particularly efficient to promote chemically active cavitation. These nuclei are destroyed to a large extent by the first pulse. The pulse itself produces nuclei, X_u, which are, however, short-lived. Their lifetime is long enough, i.e. >1 s, as pointed out above, so that trains with an interval time <1 s are still efficient. On the other hand, their lifetime is shorter than 5 s, thus the train with an interval time of 5 s is not able to produce substantial luminescence.

The existence of two types of nuclei enables one to understand also the effects of preirradiation (Figures 7b and 8b). After removal of X_n nuclei by preirradiation, a much larger number of pulses is required to build up luminescence than without preirradiation. In addition, the interval length where the pulses cease to be efficient is much shorter.

In the present work, changes in the chemical efficiency of single pulses of an ultrasonic pulse train are reported for the first time. They have to be explained by the formation and life time of bubbles acting as nuclei for chemically active cavitation. The simple theory offered can only give a qualitative explanation of the effects. The pulse experiments were carried out only at a hf-power of 70 W, i.e., on the left side of the maximum in Figure 4, where stable cavitation is believed to be dominant. The influence of the sound intensity on luminescence and chemical action by pulsed ultrasound will be reported later. Of special interest will be the very short pulses of extremely high intensity used in medicine. The first observations indicate that the activation time is very short for these pulses, but a rather long time of deactivation exists under these conditions.[10]

Acknowledgment. We thank Dr. E. Janata for help in the electronics of pulse generation. We also gratefully acknowledge the support by Deutsche Forschungsgemeinschaft.

Registry No. I^-, 20461-54-5; I_2, 7553-56-2; luminol, 521-31-3.

Chemistry of Semiconductor Clusters: A Survey of the Reactions of Si_{25}^+ Using Low-Energy Ion Beam Techniques

Martin F. Jarrold* and J. Eric Bower

Contribution from AT&T Bell Laboratories, Murray Hill, New Jersey 07974.
Received July 25, 1988

Abstract: The chemical reactions of Si_{25}^+ clusters with D_2, CH_4, O_2, C_2H_4, CO, and N_2 have been studied using low-energy ion beam techniques. The results complement our previous studies of Al_{25}^+ and allow a comparison between the reactions of metal clusters and semiconductor clusters. With D_2, CH_4, C_2H_4, and N_2, metastable adducts (arising from chemisorption on the Si_{25}^+ cluster) were directly observed, but with O_2 and CO only chemical reactions (resulting in cluster fragmentation) occur. Activation barriers for dissociative chemisorption were determined from the experimental results. The activation barriers for chemisorption of D_2, CH_4, O_2, and C_2H_4 on Si_{25}^+ are similar to those for chemisorption on Al_{25}^+. However, activation barriers for chemisorption of CO and N_2 on Si_{25}^+ are significantly larger than for chemisorption on Al_{25}^+. While there are similarities between the activation barriers for chemisorption on Si_{25}^+ and Al_{25}^+, the products of the chemical reactions are different. Si_{25}^+ shows a tendency to undergo fission in its chemical reactions, similar to the processes observed in a number of recent studies of the dissociation of the bare clusters.

We have recently reported several studies of the chemical reactions of aluminum cluster ions.[1-5] In addition to studies of the reactions with O_2 and D_2 as a function of cluster size,[1-3] we have also investigated the reactions of Al_{25}^+ with a number of simple molecules.[4,5] Al_{25}^+ was selected for detailed study because we expected its chemistry to be typical of the larger clusters where the reactivity generally changes quite slowly with cluster size. Here we describe a similar survey of the reactions of Si_{25}^+. Little is known about the structure and bonding of either Al_{25}^+ or Si_{25}^+. Detailed ab initio calculation are not available for either cluster. By analogy with the bulk materials we expect the bonding in Al_{25}^+ to be metallic with delocalized valence electrons, and the bonding in Si_{25}^+ to be covalent with localized valence electrons and directional bonding. The bonding in these two clusters is thus expected to be quite different.

In our previous work on the reactions of Al_{25}^+ we found a correlation between the activation barriers for dissociative chemisorption and the cluster HOMO → molecule LUMO promotion energies. This correlation (analogous to the one previously discussed by the Exxon group[6,7]) suggests that charge transfer (electron donation) stabilizes the transition state and lowers the activation barrier for dissociative chemisorption. We noted that other factors could also be important in determining the size of the activation barrier. The motivation for the work described in this paper was to compare the chemistry of metal and semiconductor clusters and to further probe the factors important in determining the size of the activation barriers for dissociative chemisorption on atomic clusters.

The reactions of small silicon cluster ions containing up to eight atoms have previously been studied by Mandich, Reents, and Bondybey[8-11] and Creasy, O'Keefe, and McDonald[12] using Fourier

(1) Jarrold, M. F.; Bower, J. E. *J. Chem. Phys.* **1987**, *87*, 5728.
(2) Jarrold, M. F.; Bower, J. E. *J. Am. Chem. Soc.* **1988**, *110*, 70.
(3) Jarrold, M. F.; Bower, J. E. *Chem. Phys. Lett.* **1988**, *144*, 311.
(4) Jarrold, M. F.; Bower, J. E. *J. Am. Chem. Soc.* **1988**, *110*, 6706.
(5) Jarrold, M. F.; Bower, J. E. *Chem. Phys. Lett.* **1988**, *149*, 433.
(6) Whetten, R. L.; Cox, D. M.; Trevor, D. J.; Kaldor, A. *Phys. Rev. Lett.* **1985**, *54*, 1494.
(7) Cox, D. M.; Trevor, D. J.; Whetten, R. L.; Kaldor, A. *J. Phys. Chem.* **1988**, *92*, 421.

0002-7863/89/1511-1979$01.50/0

transform ion cyclotron resonance (FT-ICR). Smalley and coworkers have surveyed the reactions between NH_3 and silicon cluster ions with up to 65 atoms also using FT-ICR.[13] These FT-ICR studies provide information on reactions at close to room temperature. In this paper we describe a low-energy ion beam study of the reactions of Si_{25}^+ with D_2, CH_4, O_2, C_2H_4, CO, and N_2. The reactions were investigated over a wide range of collision energies (from 0.2 up to 7 eV for some of the reactions), and activation barriers for dissociative chemisorption on Si_{25}^+ have been deduced from the experimental data.

Experimental Methods

The experimental apparatus and techniques have been described in detail elsewhere,[4,14,15] so only a brief description will be given here. Silicon cluster ions were generated by pulsed-laser vaporization of a silicon rod in a continuous flow of He buffer gas. After exiting the source the cluster ions were focused into a quadrupole mass spectrometer set to transmit Si_{25}^+. We have recently reported experimental evidence suggesting that the cluster ions do not contain a significant amount of excess internal energy.[4] Following mass selection the Si_{25}^+ ions were focused into a low-energy ion beam and passed through a gas cell where the neutral reagent was introduced. After exiting the gas cell the reactants and products were analyzed by a quadrupole mass spectrometer and detected with an off-axis collision dynode and dual microchannel plates. A simple three-plate retarding potential energy analyzer is located at the entrance of the second quadrupole. This was used to measure the kinetic energy of the reactant ions and calibrate the energy scale. The center of mass energy scale is accurate to within ±0.05 eV.

Silicon has several naturally occurring isotopes (Si^{28}, 92.23%; Si^{29}, 4.67%; and Si^{30}, 3.10%), and the isotope distribution for Si_{25}^+ is quite broad. Most of the experiments were performed with the first quadrupole set to select out a portion of this isotope distribution two or three mass units wide.

The main source of error with low-energy ion beam experiments is mass discrimination during product analysis and detection. We have discussed this problem in detail previously.[4] Mass discrimination becomes more serious as the mass difference between the reactants and products increases. Most of the products of the reactions studied here are quite close in mass to the reactant ions, where mass discrimination will not be a serious problem. However, a number of the secondary products (e.g., Si_{16}^+ and Si_{13}^+) and the products from collision-induced dissociation of Si_{25}^+ (Si_{15}^+) are not close in mass to the reactant ions, and for these products mass discrimination may be significant. The cross sections reported for these products should only be considered reliable to within a factor of 2.

Results

Plots of the cross sections against collision energy for the major products observed in the reactions of Si_{25}^+ with D_2, CH_4, O_2, C_2H_4, CO, and N_2 are shown in Figures 1 and 3–7, respectively. The lower half of these figures shows analogous measurements for Al_{25}^+ (taken from our previous work[2,4,5]) which are shown so that a direct comparison can be made between the reactions of Si_{25}^+ and Al_{25}^+. The points show the experimental data, and the solid lines are the results of simulations performed to deduce the true collision energy thresholds for the reactions. The simulations were performed using an assumed cross-section function and taking into account the energy spread of the ion beam and the distribution of collision energies arising from the thermal motion of the target gas. Because the mass of the neutral reagent is so much smaller than the mass of Si_{25}^+, the threshold broadening arising from thermal motion of the target gas is substantial in these experiments.

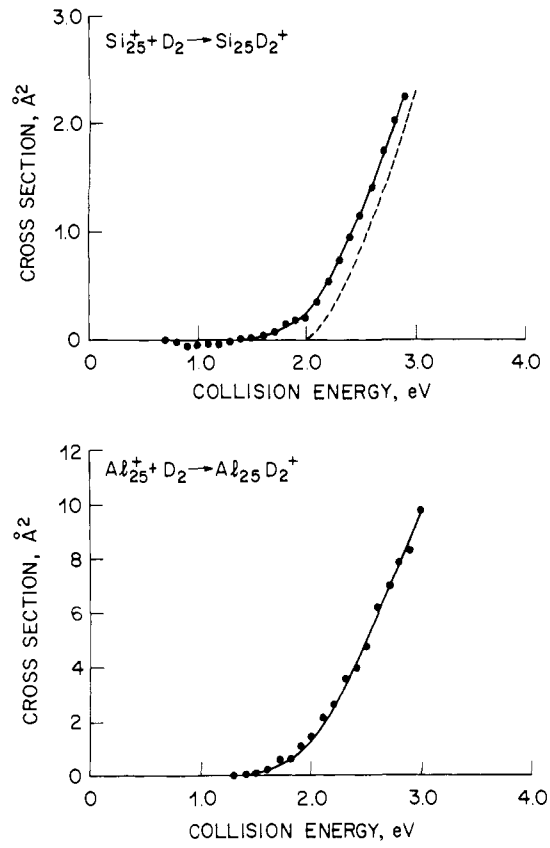

Figure 1. Plots of the cross sections against collision energy for $Si_{25}D_2^+$ (upper) and $Al_{25}D_2^+$ (lower) adduct formation in the reactions of Si_{25}^+ and Al_{25}^+ with D_2. The gas cell pressure was 0.5 mTorr. The points are the experimental data and the lines are the results of simulations (see text) to deduce the true collision energy thresholds. The data for Al_{25}^+ were taken from ref 2. The dashed line for $Si_{25}^+ + D_2$ shows a plot of the cross-section function used to simulate the experimental data.

Table I. Table Showing the Parameters Used to Model the Experimental Data for the Si_{25}^+

	simulation parameters				
reactant	E_0	A	n	m	l
D_2[a,b]	1.99	2.26	1.43		
CH_4[a]	2.91	0.059	2.32	1.82	
O_2[c]	0.29	7.24	1.96		1.00
C_2H_4	~0.0				
CO[d]	3.05	0.19	2.67		1.00
N_2[a,e]	4.96	0.099	1.50	3.04	

[a] The cross-section function used to model the experimental data was $\sigma(E) = A(E - E_0)^n \exp[-k(E - E_0,m)t]$, where E_0 is the threshold and A, n, and m are adjustable parameters. $k(E - E_0,m)$ is an analytical expression for the rate constants for unimolecular dissociation of the adduct. The expression for $k(E - E_0,m)$ was obtained by fitting a wide range of RRKM calculations. For more details see ref 2 and 4. [b] Modeled assuming no significant unimolecular dissociation of the adduct occurs. [c] The cross-section function used was $\sigma(E) = A(E - E_0)^n/E^l$, with $l = 1.00$; A, E_0, and n are adjustable parameters. Only the data for the principal product (Si_{23}^+) were modeled. For more details see ref 4. [d] Same cross-section model as for O_2 reaction. [e] n assumed to be 1.5.

The dashed line in Figure 1 shows a plot of the cross-section function used to simulate the experimental data for $Si_{25}^+ + D_2$. This represents the assumed true cross-section behavior of the reaction (i.e., the cross sections in the absence of the factors which cause threshold broadening). Details of the procedures employed to perform the simulations have been given in previous publications.[2,4] The collision energy thresholds deduced from this analysis and the other parameters used to model the experimental data are summarized in Table I along with details of the cross-section functions employed. The cross-section functions used are the

(8) Mandich, M. L.; Reents, W. D.; Bondybey, V. E. *J. Chem. Phys.* **1986**, *90*, 2315.
(9) Mandich, M. L.; Bondybey, V. E.; Reents, W. D. *J. Chem. Phys.* **1987**, *86*, 4245.
(10) Reents, W. D.; Mandich, M. L.; Bondybey, V. E. *Chem. Phys. Lett.* **1986**, *131*, 1.
(11) Reents, W. D.; Mujsce, A. M.; Bondybey, V. E.; Mandich, M. L. *J. Chem. Phys.* **1987**, *86*, 5568.
(12) Creasy, W. R.; O'Keefe, A.; McDonald, J. R. *J. Phys. Chem.* **1987**, *91*, 2848.
(13) Elkind, J. L.; Alford, J. M.; Weiss, F. D.; Laaksonen, R. T.; Smalley, R. E. *J. Chem. Phys.* **1987**, *87*, 2397.
(14) Jarrold, M. F.; Bower, J. E.; Kraus, J. S. *J. Chem. Phys.* **1987**, *86*, 3876.
(15) Jarrold, M. F.; Bower, J. E. *J. Phys. Chem.* **1988**, *92*, 5702.

Table II. Thresholds Deduced from the Simulations of the Experimental Data

reactant	Si_{25}^+	Al_{25}^+ [a]
D_2	2.0 ± 0.3	2.0 ± 0.2
CH_4	2.9 ± 0.3	3.5 ± 0.3
O_2	0.3 ± 0.3	0.5 ± 0.3
C_2H_4	~0.0	~0.0
CO	3.1 ± 0.5	1.9 ± 0.3
N_2	5.0 ± 0.8	3.5 ± 0.3

[a] The data for Al_{25}^+ were taken from ref 2, 4, and 5.

simplest physically realistic models able to account for the experimental data. Owing to the relatively large amount of threshold broadening present in these experiments, the choice of the correct cross-section function is important. While we try to model the cross sections over a wide collision energy range, this is not a guarantee that the cross-section function is correct in the important threshold region.

A. $Si_{25}^+ + D_2$. D_2 chemisorbs on Si_{25}^+ to give a $Si_{25}D_2^+$ adduct which is directly observable. Cross sections for $Si_{25}D_2^+$ adduct formation are shown in Figure 1 plotted as a function of collision energy. In the low-pressure environment of the gas cell, the adduct is not stabilized by further collisions and so has sufficient energy to dissociate back to reactants. However, the adduct is metastable and survives long enough (>4 μs) to reach the mass spectrometer and be detected because of the large number of internal degrees of freedom in the cluster.

Besides the $Si_{25}D_2^+$ adduct no other products were observed. Owing to the large laboratory energies employed in these studies (because D_2 is so light), the lighter products, if any are formed, will be discriminated against. At the highest center-of-mass collision energy studied (3 eV), products lighter than Si_{10}^+ would not be detectable. Furthermore, because of the isotope distribution, it is difficult to detect small amounts of products very close in mass to the reactant ions. So we would not be able to detect a small amount of $Si_{25}D^+$ if it were formed. Under the conditions employed to record the data shown in Figure 1, the $Si_{25}D_2^+$ product peak sits on the edge of the much larger Si_{25}^+ peak in the mass spectrum. As a consequence the threshold region (where the $Si_{25}D_2^+$ signal is small) is quite noisy.

As can be seen from Figure 1 the cross sections for $Si_{25}D_2^+$ formation show an apparent threshold at collision energies around 1.5 eV and then rise to around 2.5 Å^2 at a collision energy of 3 eV. The shape of the cross-section plot for Si_{25}^+ is remarkably similar to that for Al_{25}^+ shown in the lower half of Figure 1, though the cross sections for Al_{25}^+ are around four times larger. A possible explanation for the smaller cross sections observed for Si_{25}^+ is that steric constraints (the orientation of the D_2 with respect to the cluster and the site where the D_2 strikes the cluster surface) are more severe for Si_{25}^+ than for Al_{25}^+. The lines drawn through the data in Figure 1 are the results of a simulation to deduce the true collision energy thresholds. The thresholds and other parameters used to model the experimental data are summarized in Table I and the thresholds for Si_{25}^+ and Al_{25}^+ are compared in Table II. The collision energy threshold for adduct formation can be related to the activation barriers for chemisorption. Clearly the activation barriers for chemisorption of D_2 on Si_{25}^+ and Al_{25}^+ are similar. In their study of the reactions of Si_{2-6}^+ using FT-ICR, Creasy and co-workers[12] found no reaction with D_2. It is not clear if this result indicates that there is a significant activation barrier for chemisorption of D_2 on Si_{2-6}^+.

B. $Si_{25}^+ + CH_4$. Si_{25}^+ reacts with CH_4 to give three main products: the $Si_{25}CH_4^+$ adduct, $Si_{15}CH_4^+$, and Si_{15}^+. Owing to the isotope distribution it was not possible to resolve product ion masses separated by 1 amu, so there could be small components of other masses present. For example, the $Si_{15}CH_4^+$ peak could contain a small component of $Si_{15}CH_3^+$. Figure 2 shows a plot of the relative intensities of the products against the gas cell pressure. The data shown in Figure 2 were recorded with a collision energy of 6 eV. All the products show a nonlinear pressure dependence. The intensity of the $Si_{25}CH_4^+$ product begins to level off at the higher pressures studied. This probably arises from dissociation of the adduct caused by collisional activation in secondary collisions. The intensities of the other two products show a faster than linear increase with pressure. The Si_{15}^+ product shows a close to quadratic dependence on pressure. Si_{15}^+ is the dominant product from the photodissociation[16] of Si_{25}^+ and from the collision-induced dissociation[15] of Si_{25}^+ by argon, and probably arises mainly from collision-induced dissociation here as well. The close to quadratic pressure dependence observed for this product suggests that multiple collisions are required to cause dissociation of Si_{25}^+ even at a collision energy of 6 eV. This result does not imply that the dissociation energy of Si_{25}^+ is more than 6 eV because a substantial amount of excess energy is required to cause such a large cluster to dissociate (in ~7 μs) before reaching the mass spectrometer. The $Si_{15}CH_4^+$ product probably arises from dissociation of the $Si_{25}CH_4^+$ adduct. Apparently the dominant dissociation channel of both Si_{25}^+ and $Si_{25}CH_4^+$ is loss of Si_{10}. Though multiple collision processes are clearly important in the 0.2–1-mTorr pressure regime discussed above, it should be noted that, when the gas cell length (2.5 cm) is taken into account, these pressures correspond to target gas densities of only 1.7–8.8 × 10^{13} molecules/cm^2. Clearly the cross sections for collisional activation are large; we estimate ~10–50 Å^2, which is much larger than the reaction cross sections. In our previous work[4] on Al_{25}^+ we came to the same conclusion.

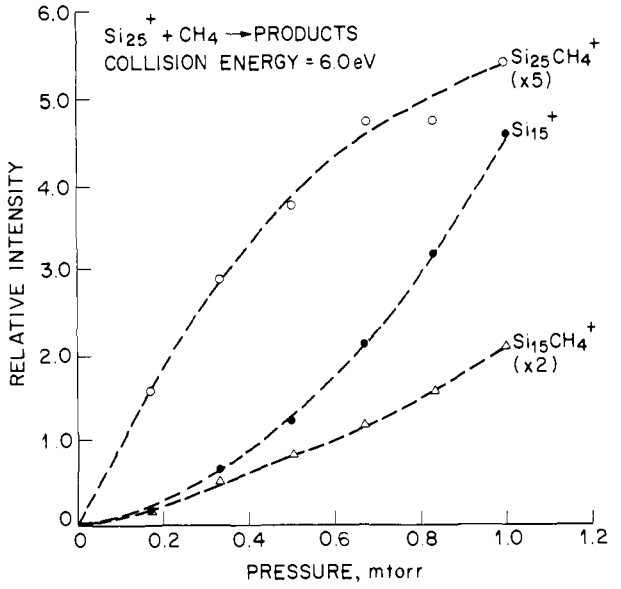

Figure 2. Plot of the gas cell pressure dependence of the intensities of the main products from the reaction between Si_{25}^+ and CH_4. The collision energy was 6 eV. The dashed lines drawn through the data are only guides.

The upper half of Figure 3 shows a plot of the cross sections for the products from the reaction between Si_{25}^+ and CH_4 against collision energy, recorded with a gas cell pressure of 0.5 mTorr. The $Si_{25}CH_4^+$ adduct appears to have the lowest energy threshold. The threshold for $Si_{15}CH_4^+$ is around 1 eV higher in energy. The lines drawn through the experimental data are the results of simulations to deduce the true collision energy thresholds. The measured thresholds are not significantly influenced by collisional activation in secondary collisions. It is apparent from Figure 3 and Table II that the thresholds for formation of $Si_{25}CH_4^+$ and $Al_{25}CH_4^+$ are quite similar. However, $Si_{25}CH_4^+$ fragments by loss of Si_{10} to give $Si_{15}CH_4^+$, but $Al_{25}CH_4^+$ fragments by loss of AlH or $AlCH_3$ to give $Al_{24}CH_3^+$ and $Al_{24}H^+$, respectively.

C. $Si_{25}^+ + O_2$. In the reaction between Si_{25}^+ and O_2 three main products were found: Si_{23}^+, Si_{16}^+, and Si_{13}^+. No $Si_{25}O_2^+$ adduct was observed. Figure 4 shows a plot of the cross sections for the products against collision energy. Note that this is an efficient reaction and the cross sections are quite large. At a collision energy

(16) Zhang, Q.-L.; Liu, Y.; Curl, R. F.; Tittel, F. K.; Smalley, R. E. *J. Chem. Phys.* **1988**, *88*, 1670.

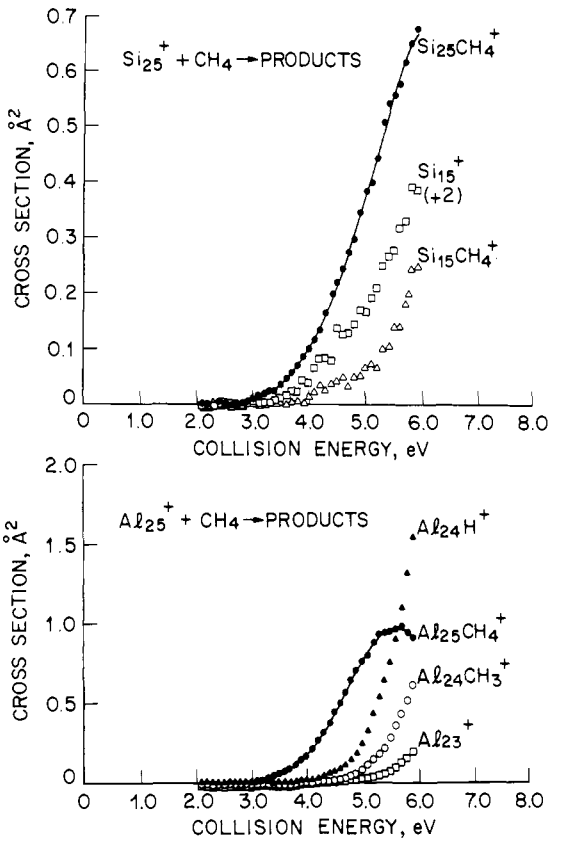

Figure 3. Plots of the cross sections against collision energy for the products observed in the reactions between Si_{25}^+ and CH_4 (upper), and between Al_{25}^+ and CH_4 (lower). The gas cell pressure was 0.5 mTorr for the Si_{25}^+ data and 0.25 mTorr for Al_{25}^+. The points are the experimental data and the lines are the results of simulations to deduce the true collision energy thresholds. The data for Al_{25}^+ were taken from ref 4.

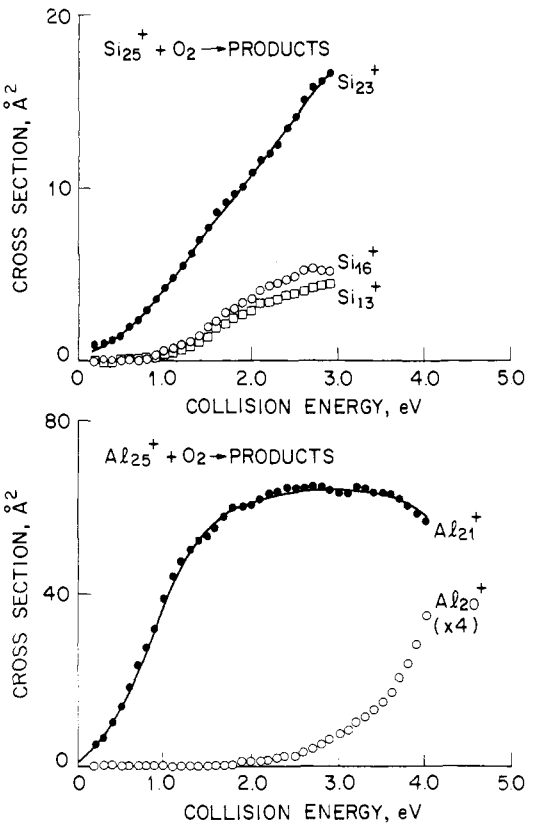

Figure 4. Plots of the cross sections against collision energy for the products observed in the reactions between Si_{25}^+ and O_2 (upper), and between Al_{25}^+ and O_2 (lower). The gas cell pressure was 0.5 mTorr for the Si_{25}^+ data and 0.25 mTorr for Al_{25}^+. The points are the experimental data and the lines are the result of simulations to deduce the true collision energy thresholds. The data for Al_{25}^+ were taken from ref 4.

of 3 eV all three products showed a close-to-linear variation with gas cell pressure, up to a pressure of 1.0 mTorr. The reactions between silicon cluster ions with up to six atoms and O_2 have been studied by Creasy, O'Keefe, and McDonald using FT-ICR.[12] The main product they found was loss of two silicon atoms to give Si_{n-2}^+. The neutral products are presumably either two SiO molecules or an Si_2O_2 species. The main product found for Si_{25}^+ is also Si_{n-2}^+. Si_{16}^+ and Si_{13}^+ are the main products from the collision-induced dissociation of Si_{23}^+ by argon.[15] So the Si_{16}^+ and Si_{13}^+ products probably arise from further dissociation of the Si_{23}^+ product. However, since the products all show a close-to-linear gas cell pressure dependence, the Si_{16}^+ and Si_{13}^+ products, in this case, probably arise mainly from further fragmentation of Si_{23}^+ excited in the reaction with oxygen, rather than from collisional activation.

There are obvious similarities between the $Si_{25}^+ + O_2$ and $Al_{25}^+ + O_2$ reactions. With Al_{25}^+ the main product is Al_{21}^+, arising from loss of two Al_2O molecules. At higher collision energies some Al_{20}^+ arises from further fragmentation of the Al_{21}^+ product. As can be seen from Figure 4 the $Al_{25}^+ + O_2$ reaction occurs with greater probability than the $Si_{25}^+ + O_2$ reaction. But the collision energy thresholds for the reactions are quite similar. The thresholds deduced from the simulations of the experimental data (see Table I) are shown in Table II. It appears that the Si_{25}^+ reaction may have a slightly lower threshold. In the simulation of the Si_{25}^+ data only the main product (Si_{23}^+) was modeled. We were unable to obtain a satisfactory fit to the total reaction cross sections; this might be considered evidence that the other products (Si_{16}^+ and Si_{13}^+) arise from a mechanism different from simple fragmentation of the Si_{23}^+ product as suggested above.

In their FT-ICR study of the reactions of Si_{2-6}^+ with O_2 Creasy and co-workers[12] found that the reaction rates were slow and decreased with cluster size. Noting that the reactions were very exothermic (by ~2–3 eV if the products are two SiO molecules and 1.93 eV[17] more exothermic if the product is Si_2O_2), they suggested that there must be an activation barrier associated with O–O bond breaking and Si–O bond formation. There is no information available for the binding energy of a Si atom to Si_{25}^+, however, even using the bulk cohesive energy,[18,19] the reaction of Si_{25}^+ with oxygen is exothermic by at least 2 eV. So it is reasonable to associate the small activation barrier we found for the reaction of Si_{25}^+ with O_2 with chemisorption of O_2 onto the Si_{25}^+ cluster. Once the O_2 is dissociatively chemisorbed, the $Si_{25}O_2^+$ species dissociates to give the observed products. The overall reaction is presumably sufficiently exothermic that the $Si_{25}O_2^+$ adduct dissociates before it reaches the mass spectrometer (indicating a lifetime <5 μs). The activation barrier of 0.3 eV deduced from our low-energy ion beam studies is large enough that the reaction at room temperature would probably be immeasurably slow. This is consistent with the fall in the reaction rates observed by Creasy and co-workers[12] over the cluster size range Si_2^+–Si_6^+.

Despite the similarities in the thresholds for the reactions of Al_{25}^+ and Si_{25}^+ with O_2, it is apparent from Figure 3 that above threshold the cross sections for Si_{25}^+ and Al_{25}^+ show a different dependence on collision energy. With Al_{25}^+ the cross sections increase rapidly and then level off at a value which is a substantial fraction (~50%) of the geometric cross section. With Si_{25}^+ the reaction cross sections increase much more slowly. One possible

(17) Zmbov, K. F.; Ames, L. L.; Margrave, J. L. *High Temp. Sci.* **1973**, *5*, 235. Snyder, L. C.; Raghavachari, K. *J. Chem. Phys.* **1984**, *80*, 5076.

(18) Using the bulk cohesive energy for $D(Si_{n-1}\text{–}Si)$ (for $n \sim 25$) is reasonable because several theoretical calculations[19] suggest that with silicon clusters the bulk cohesive energy is quickly approached.

(19) See, for example: Raghavachari, K.; Logovinsky, V. *Phys. Rev. Lett.* **1985**, *55*, 2853. Tomanek, D.; Schluter, M. A. *Phys. Rev. Lett.* **1986**, *56*, 1055; Raghavachari, K.; Rohlfing, C. M. *Chem. Phys. Lett.* **1988**, *143*, 428.

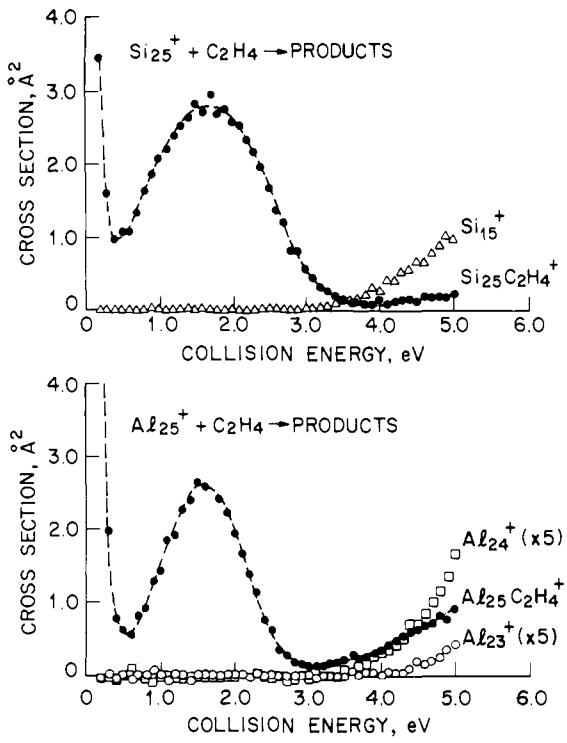

Figure 5. Plots of the cross sections against collision energy for the products observed in the reactions between Si_{25}^+ and C_2H_4 (upper), and between Al_{25}^+ and C_2H_4 (lower). The gas cell pressure was 0.5 mTorr. The points are the experimental data. The dashed lines drawn through the points for adduct formation are only a guide. The data for Al_{25}^+ were taken from ref 5.

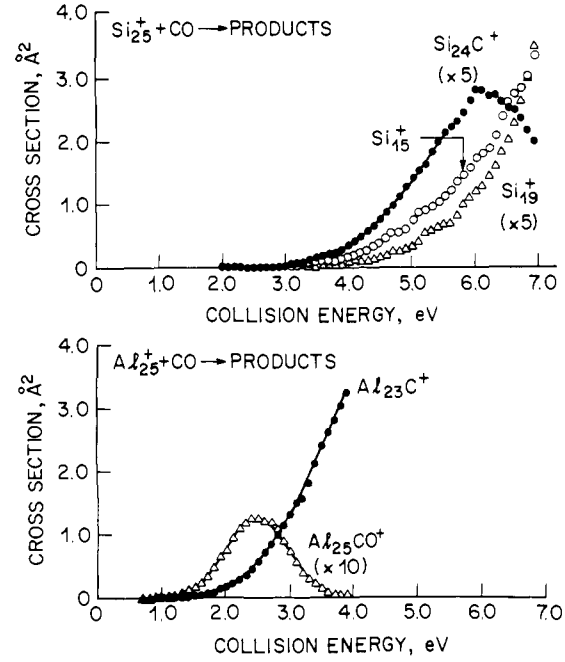

Figure 6. Plots of the cross sections against collision energy for the products observed in the reactions between Si_{25}^+ and CO (upper), and between Al_{25}^+ and CO (lower). The gas cell pressure was 0.5 mTorr. The points are the experimental data and the lines are the result of simulations to deduce the true collision energy thresholds. The data for Al_{25}^+ were taken from ref 4.

explanation for this behavior is steric constraints. With Al_{25}^+ steric effects are relatively unimportant. Once sufficient energy is available to surmount the activation barrier, chemisorption occurs with high efficiency. With Si_{25}^+ steric effects (the orientation of the O_2 molecule with respect to the cluster surface, and the site where the oxygen molecule strikes the cluster) may be more important, and the chemisorption efficiency increases more slowly above threshold. The origin of the difference between Al_{25}^+ and Si_{25}^+ could be the differences in the bonding in the clusters. With Si_{25}^+ directional covalent bonding is expected, and it is possible that a site with specific coordination numbers and geometry is required for chemisorption of oxygen.

D. $Si_{25}^+ + C_2H_4$. We have recently reported that the chemisorption of C_2H_4 on Al_{25}^+ is a remarkably complicated process.[5] It appears that three different types of $Al_{25}C_2H_4^+$ adduct are formed over different collision energy ranges. Surprisingly, Si_{25}^+ behaves in essentially the same way. The data are shown in Figure 5. At the lowest collision energy studied (0.2 eV) C_2H_4 sticks to Si_{25}^+, yielding a $Si_{25}C_2H_4^+$ adduct. The cross sections for adduct formation drop as the collision energy is raised, suggesting that there is no significant activation barrier to forming this adduct. The falloff in the adduct cross sections with increasing collision energy is probably due to adduct dissociation. These results suggest that this adduct is quite weakly bound since a small amount of extra energy is sufficient to cause dissociation before the adduct reaches the mass spectrometer (in $\sim$15 μs). As no other products are observed in this collision energy range, the adduct presumably dissociates by simple desorption of an intact C_2H_4 molecule.

As the collision energy is raised above 0.5 eV, the cross sections for adduct formation begin to rise again. This must be due to the formation of a different type of adduct. The cross sections for this adduct peak at around 1.7 eV and then begin to fall, presumably because sufficient energy is now available for a significant fraction of the adduct to dissociate before it can be detected. No other products are observed in this collision energy range so the adduct presumably dissociates by desorbing an intact C_2H_4 molecule. Above a collision energy of 4 eV, the cross sections for adduct formation rise again, indicating the formation of yet another type of adduct. In this collision energy range another product is observed: Si_{15}^+. This probably arises from collision-induced dissociation of Si_{25}^+ and/or the $Si_{25}C_2H_4^+$ adduct. The intensity of the Si_{15}^+ product shows a close-to-quadratic dependence on the gas cell pressure, indicating that it arises from a multiple-collision process.

As can be seen from Figure 5 there is a strong similarity between the reactions of Si_{25}^+ and Al_{25}^+ with C_2H_4. One significant difference is in the amount of the highest energy adduct formed. Substantially less of this is formed from Si_{25}^+ than from Al_{25}^+. C_2H_4 is known to give rise to a number of different products on metal surfaces,[20] and in our previous work on the reactions of Al_{25}^+ with C_2H_4 we suggested that the three different types of adduct formed corresponded to different structures for the C_2H_4 species on the cluster surface. The observation of the same behavior with Si_{25}^+ supports this assignment: an alternative explanation is that different sites on the clusters are responsible, but it would be hard to argue that this could occur for both Al_{25}^+ and Si_{25}^+, which almost certainly have different structures. Unfortunately, our experiments provide essentially no information on what the structures of the different adducts might be.

E. $Si_{25}^+ + CO$. CO dissociatively chemisorbs on Al_{25}^+ yielding an $Al_{25}CO^+$ adduct. We found no evidence for $Si_{25}CO^+$ adduct formation with Si_{25}^+. However, we did observe several other products: $Si_{24}C^+$, Si_{19}^+, and Si_{15}^+. The Si_{15}^+ product probably arises mainly from collision-induced dissociation, but the other products must arise from a chemical reaction. As can be seen from Figure 6, the product with the lowest energy threshold is $Si_{24}C^+$. This product probably arises from dissociative chemisorption of CO on the Si_{25}^+ cluster followed by loss of an SiO molecule from the adduct. The cross sections for $Si_{24}C^+$ show a threshold at around 3 eV, rise to a maximum at around 6 eV, and then start to fall. Coincident with the fall in the cross sections for $Si_{24}C^+$, the cross sections for Si_{19}^+ increase sharply. This result suggests that the $Si_{24}C^+$ product is fragmenting further to give

(20) See, for example: Bertolini, J. C.; Massardier, J. In *The Chemical Physics of Solid Surfaces and Heterogeneous Catalysis*. Vol. 3. *Chemisorption Systems*; King, D. A., Woodruff, D. P., Eds.; Elsevier: Amsterdam, 1984.

Si_{19}^+. The neutral product associated with the Si_{19}^+ ion is presumably Si_5C which is an analogue of the stable Si_6 cluster. In the collision-induced dissociation of silicon cluster cations[15] loss of Si_6 is an important process for clusters with 12–17 atoms. For clusters with 18–26 atoms loss of Si_{10} is the dominant process. With $Si_{24}C^+$, the $Si_{19}^+ + Si_5C$ products are presumably more stable than those arising from loss of Si_{10} (or Si_9C). It is also worth noting that $Si_{18}C^+ + Si_6$ were not observed as products. Apparently of the options discussed, the C atom is located in the smallest cluster: Si_5C.

Though $Al_{25}CO^+$ was observed in the reaction of Al_{25}^+ with CO, no adduct was observed in the reaction of Si_{25}^+. However, as can be seen from Figure 6, the cross sections for the $Al_{25}CO^+$ adduct are small, and it is only observed over a relatively narrow collision energy range. The main product observed is $Al_{23}C^+$ which presumably arises from loss of Al_2O from the $Al_{25}CO^+$ adduct. If the activation barrier for chemisorption of CO on Al_{25}^+ was slightly larger, it is doubtful if we would have been able to directly observe the $Al_{25}CO^+$ adduct, because it would have dissociated (to $Al_{23}C^+ + Al_2O$) before we could have detected it. Presumably the $Si_{25}CO^+$ adduct dissociates before it can be detected. If this is so, then the activation barrier for dissociative chemisorption of CO on Si_{25}^+ can be deduced from the threshold for $Si_{24}C^+$ formation. Note, however, that unlike the thresholds for adduct formation, the thresholds for the formation of products such as $Si_{24}C^+$ cannot in general be unambiguously related to activation barriers for chemisorption because there could be an activation barrier on going from the adduct to the products. The lines in Figure 6 shows the simulations to deduce the true collision energy threshold. In the case of $Si_{24}C^+$ we only modeled the cross sections up to a collision energy of 5.5 eV, since above 6.0 eV it is clear that this product is depleted by further dissociation to Si_{19}^+. The activation barrier for chemisorption of CO on Si_{25}^+ deduced in this way was 3.1 ± 0.5 eV, which is considerably larger than the activation barrier for chemisorption on Al_{25}^+ (1.9 ± 0.3 eV).

F. $Si_{25}^+ + N_2$. The data for the reactions with N_2 are shown in Figure 7. With Si_{25}^+ a $Si_{25}N_2^+$ adduct is observed. The other main product is Si_{15}^+ which probably arises mainly from collision-induced dissociation of Si_{25}^+. The cross sections for $Si_{25}N_2^+$ adduct formation are very small (note the ×10 scale factor in Figure 7). From a simulation of the experimental data we deduced an activation barrier for chemisorption of N_2 onto Si_{25}^+ of 5.0 ± 0.8 eV. Because of the fairly large amount of scatter in the experimental points, we experienced difficulty in getting the least-squares procedure used in the simulation to converge, and it was necessary to assume a more restrictive cross-section model (see Table I) than employed for the Al_{25}^+ reaction. The relatively large error bars given for the threshold for adduct formation reflect these difficulties. However, despite these conservative error limits it is clear from Table II and from Figure 7 that the threshold for chemisorption of N_2 on Si_{25}^+ (5.0 ± 0.8 eV) is considerably larger than for chemisorption on Al_{25}^+ (3.5 ± 0.3 eV).

Discussion

A. Comparison of the Reactions of Si_{25}^+ with Silicon Surface Chemistry. Here we compare the chemistry of Si_{25}^+ with the chemistry observed on silicon surfaces. The interaction of hydrogen with silicon has been studied quite extensively[21,22] because it has been considered a prototype for the chemistry of semiconductor surfaces. Molecular hydrogen does not chemisorb on silicon at room temperature, although atomic hydrogen does.[21,22] We are not aware of any experimental measurement of the activation barrier for chemisorption of molecular hydrogen on silicon. In their theoretical study of the recombination and desorption of H_2 on Si(111), NoorBatcha, Raff, and Thompson[22] determined

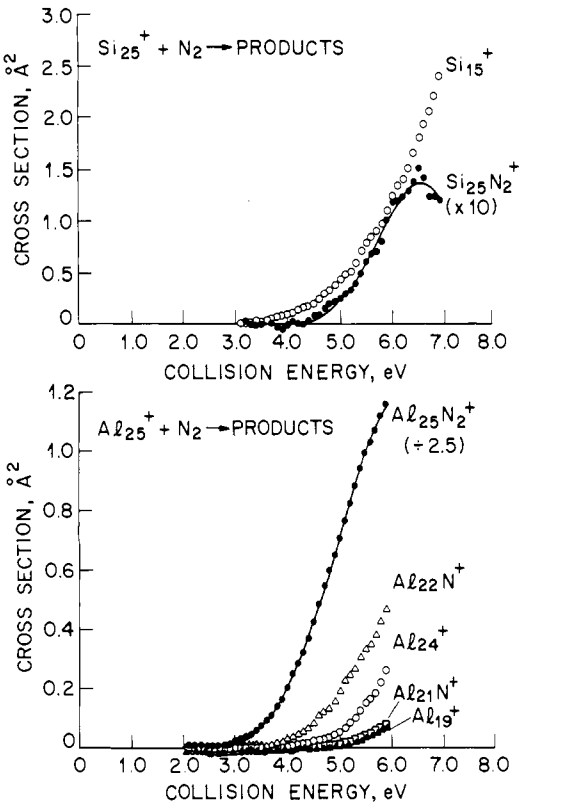

Figure 7. Plots of the cross sections against collision energy for the products observed in the reactions between Si_{25}^+ and N_2 (upper), and between Al_{25}^+ and N_2 (lower). The gas cell pressure was 0.5 mTorr. The points are the experimental data and the lines are the result of simulations to deduce the true collision energy thresholds. The data for Al_{25}^+ were taken from ref 4.

an activation barrier of 0.81 eV for dissociative chemisorption of H_2, and an activation barrier of 0.61 eV for molecular adsorption. The threshold of 2.0 eV determined in this work for the chemisorption of D_2 on Si_{25}^+ is almost certainly the activation barrier for dissociative chemisorption since it is unlikely that a weakly bound adduct arising from molecular chemisorption would survive long enough to be directly observed. In any case the activation barrier for Si_{25}^+ is substantially larger than for the theoretical value for the bulk surface. We found the same result for Al_{25}^+, where again there have been no direct experimental measurements for chemisorption of H_2 on aluminum surfaces, but theory provides an estimate of 1.3 eV[23] and we found a threshold for chemisorption on the cluster of 2.0 eV.

CH_4 does not appear to react with silicon surfaces at room temperature.[24] This is consistent with the large activation barrier observed for the cluster.

The oxidation of silicon surfaces by oxygen has been extensively studied.[25] While the details remain controversial, it is clear that the surface readily oxidizes to ultimately yield an oxidized surface layer. We found a small activation barrier (0.3 eV) for the reaction of Si_{25}^+ with oxygen, and, unlike the bulk where an oxidized surface layer is formed, oxygen etches the Si_{25}^+ to Si_{23}^+. This occurs because the silicon cluster does not have a large lattice to accomodate the exothermicity arising from chemisorption of oxygen. At high temperatures (>975 K) desorption of SiO has been observed in the oxidation of silicon surfaces.[26]

(21) For examples of experimental work, see: Ibach, H.; Rowe, J. E. *Surf. Sci.* **1974**, *43*, 481. Kobayashi, H.; Edamoto, K.; Onchi, M.; Nishijima, M. *J. Chem. Phys.* **1983**, *78*, 7429. For examples of theoretical work, see: Appelbaum, J. A.; Hamann, D. R. *Phys. Rev. Lett.* **1975**, *34*, 806. Allan, D. C.; Mele, E. J. *Phys. Rev. B* **1985**, *31*, 5565.

(22) NoorBatcha, I.; Raff, L. M.; Thompson, D. L. *J. Chem. Phys.* **1985**, *83*, 1382.

(23) Johansson, P. K. *Surf. Sci.* **1981**, *104*, 510.

(24) Creasy, W. R.; McElvany, S. W. *Surf. Sci.*, in press.

(25) For examples of experimental work, see: Kasupke, N.; Henzler, M. *Surf. Sci.* **1980**, *92*, 407. Edamoto, K.; Kubota, Y.; Kobayashi, H.; Onchi, M.; Nishijima, M. *J. Chem. Phys.* **1985**, *83*, 428. For examples of theoretical work, see: Bhandia, A. S.; Schwarz, J. A. *Surf. Sci.* **1981**, *108*, 587. Redondo, A.; Goddard, W. A.; Swarts, C. A.; McGill, T. C. *J. Vac. Sci. Technol.* **1981**, *19*, 498.

(26) D'Evelyn, M. P.; Nelson, M. M.; Engel, T. *Surf. Sci.* **1987**, *186*, 75.

C_2H_4 chemisorbs on silicon at room temperature.[27,28] The available data are consistent with molecular chemisorption and a strongly bound π-bonded adsorption state.[28] Above room temperature (660 K) desorption of H_2 is observed, suggesting that the C_2H_4 dissociates on the surface.[27] We found no significant activation barrier for chemisorption of C_2H_4 on Si_{25}^+, but we found no evidence for desorption of H_2 from the $Si_{25}C_2H_4^+$ adduct over the entire energy range studied (0.2–5.0 eV). It is possible that a small amount (<10% of $Si_{25}C_2H_4^+$ signal) of $Si_{25}C_2H_2^+$ is present and obscured in the mass spectrum by the tail on the $Si_{25}C_2H_4^+$ peak (which is due to the isotope distribution). Another interesting possibility is that desorption of H_2 (from the cluster or from the bulk surface) requires more than one adsorbed C_2H_4 molecule; this would be true if C_2H_4 absorbed to give $-C_2H_3$ and $-H$. Desorption of H_2 was observed for collision energies above 3 eV for Al_{25}^+.

N_2 and CO do not adsorb on silicon surfaces at room temperature; however, both will chemisorb under the influence of an electron beam.[29] This is consistent with our observations for Si_{25}^+ where we find that both CO and N_2 show large activation barriers for chemisorption on the cluster.

In summary, of the molecules we have studied only O_2 and C_2H_4 chemisorb on bulk silicon at room temperature. As can be seen from Table II, O_2 and C_2H_4 have the smallest activation barriers for chemisorption on Si_{25}^+, so there appears to be a qualitative correlation between the chemistry observed for Si_{25}^+ and the chemistry which occurs on bulk silicon. Of the molecules studied only O_2 and C_2H_4 react with bulk aluminum at room temperature; thus it appears that the similarity between the activation barriers for chemisorption on Si_{25}^+ and Al_{25}^+ is also displayed to some extent by the bulk surfaces of these materials.

B. What Determines the Size of the Activation Barriers? In our previous work on the reactions of Al_{25}^+ we found a qualitative correlation between the activation barriers and the cluster HOMO → molecule LUMO promotion energies.[4] This correlation suggests that charge transfer (electron donation) stabilizes the transition state and lowers the activation barriers for dissociative chemisorption. It might be thought that charge transfer from a positively charged ion to a neutral molecule is not a favored process. However, the cluster is large and the charge extensively delocalized; furthermore, charge transfer from the cluster's HOMO to the molecule's LUMO could be compensated for by back donation from the molecule's HOMO to the cluster's LUMO. In recent calculations of the activation barriers for chemisorption of D_2 onto Al_6^-, Al_6, and Al_6^+, Upton and co-workers[30] found that the degree transfer at the transition state was not strongly influenced by the presence of the charge. As noted in the Introduction, one of the reasons we performed the work described in this paper was to compare the chemistry of Si_{25}^+ with that of Al_{25}^+. We expect the chemical bonding and geometric structures of Si_{25}^+ and Al_{25}^+ to be dramatically different (directional covalent for Si_{25}^+ and metallic for Al_{25}^+), so a strong similarity between the activation barriers for chemisorption on Si_{25}^+ and Al_{25}^+ would provide convincing evidence that charge-transfer stabilization of the transition state is an important factor in determining the size of the activation barrier. In Figure 8 we compare the activation energies determined for Al_{25}^+ and Si_{25}^+ with the cluster HOMO → molecule LUMO promotion energies. The energies of the orbitals were taken from ref 31 and the cluster HOMO energy is taken to be the second ionization potential of the cluster. We estimate that the second ionization potentials of Si_{25} and Al_{25} are probably both around 8.7 eV.[14,32-34] The data for C_2H_4 are plotted separately from the rest of the molecules studied. We have done this because we are fairly confident that the activation barriers measured for D_2, CH_4, O_2, CO, and N_2 are for dissociative chemisorption. With C_2H_4 several different adducts appear to be formed over different collision energy ranges. While we cannot be sure, it seems likely that at least the adduct which occurs at the lowest collision energies arise from molecular chemisorption rather than dissociative chemisorption. Furthermore, as can be seen from Figure 8 the HOMO of C_2H_4 lies considerably higher in energy than the HOMO's of the rest of the molecules studied, so for C_2H_4 molecule HOMO → cluster LUMO donor interactions could be much more important than for the other molecules.

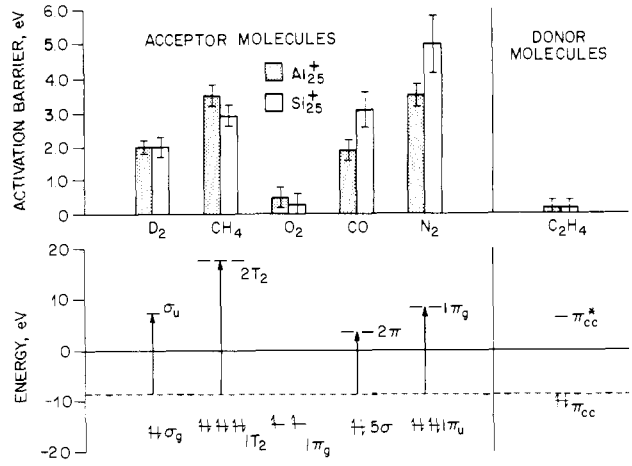

Figure 8. Diagram showing a comparison between the activation barriers measured for chemisorption of Si_{25}^+ and Al_{25}^+ and the cluster HOMO → molecule LUMO promotion energies. The orbital energies were taken from ref 31 and the cluster HOMO is assumed to be given by the second ionization potential (see text).

As can be seen from Figure 8, there is a rough qualitative correlation between the activation barriers for dissociative chemisorption of D_2, CH_4, O_2, CO, and N_2 on Al_{25}^+ and Si_{25}^+ and the cluster HOMO → molecule LUMO promotion energies, but we need to be careful about interpreting this result because different types of orbitals are involved. With D_2 and CH_4 we are dealing with σ^* orbitals. The larger activation barrier for chemisorption of CH_4 correlates with the higher energy LUMO of this molecule. Oxygen is a triplet with an unfilled HOMO so a small activation barrier would be expected. For CO and N_2 the LUMO is a π^* orbital and CO with the lower energy LUMO has the smaller activation barrier for chemisorption on both Si_{25}^+ and Al_{25}^+. These results apparently confirm the idea that charge-transfer stabilization of the transition state is a factor in determining the size of the activation barriers. However, this is certainly not the only factor. In the above discussion, we have ignored symmetry requirements. The strength of the bonds being broken and formed is also probably important.[35] Shustorovitch[36] has incorporated this idea into a simple model for dissociative chemisorption on metal surfaces. In our previous work on Al_{25}^+ we attempted to compare the activation barriers to the predictions of the model of Shustorovitch. This requires knowledge of the binding energies of the molecules to the clusters, which have not been measured.

(27) Klimesch, P.; Meyer, G.; Henzler, M. *Surf. Sci.* **1984**, *137*, 79.
(28) Piancastelli, M. N.; Kelly, M. K.; Kilday, D. G.; Margaritondo, G.; Frankel, D. J.; Lapeyre, G. J. *Phys. Rev. B* **1987**, *35*, 1461.
(29) Schrott, A. G.; Fain, S. C. *Surf. Sci.* **1981**, *111*, 39. Ekwelundu, E.; Ignatiev, A. *Surf. Sci.* **1987**, *179*, 119.
(30) Upton, T. H.; Cox, D. M.; Kaldor, A. *Physics and Chemistry of Small Clusters*; Jena, P., Rao, B. K., Khanna, S. N., Eds.; Plenum: New York, 1987.
(31) Jorgensen, W. L.; Salem, L. *The Organic Chemist's Book of Orbitals*; Academic: New York, 1973.
(32) Second ionization potentials have not been measured for Al_{25} or Si_{25}. However, from the work of Brechignac and co-workers[33] we estimate that the second ionization potentials are 3 eV larger than the first. There is only limited information available on the first ionization potentials of Al_{25} and Si_{25}. The ionization potential of Al_{25} has been indirectly estimated,[14] and for Si_{25} the ionization potential has been coarsely bracketed.[34] From this work it appears that the ionization potentials of Si_{25} and Al_{25} are both around 5.7 ± 1.0 eV.
(33) Brechignac, C.; Broyer, M.; Cahuzac, Ph.; Delacretaz, G.; Labastie, P.; Woste, L. *Chem. Phys. Lett.* **1985**, *118*, 174.
(34) Trevor, D. J.; Cox, D. M.; Reichmann, K. C.; Brickman, R. O.; Kaldor, A. *J. Phys. Chem.* **1987**, *91*, 2598.
(35) Hammond, G. S. *J. Am. Chem. Soc.* **1955**, *77*, 334.
(36) Shustorovitch, V. *Surf. Sci. Rep.* **1986**, *6*, 1.

With Al_{25}^+ we made some rough estimates of the binding energies, and there appeared to be a qualitative correlation between the predictions of Shustorovitch's model and the measured activation barriers. With Si_{25}^+ any estimates of the binding energies we can make appear so unreliable that a meaningful comparison cannot be made at this time. Another factor that is certainly important in determining the size of activation barriers for dissociative chemisorption on atomic clusters is the electronic structure of the metal. Transition metal clusters with a partially filled d shell chemisorb hydrogen with no significant activation barrier.[6,37] With aluminum and silicon clusters there are substantial activation barriers. Finally, there is the role of geometric structure. Several recent papers have argued that geometric structure or shape are important factors in controlling the reactivity of atomic clusters.[38,39] Geometry and electronic structure are intimately related and their effects difficult to separate, but the role of geometry is probably considerably more subtle than the other factors we have discussed above.

As can be seen from Figure 8, although the activation barriers for chemisorption on Si_{25}^+ and Al_{25}^+ show the same qualitative trends, there are significant differences. The activation barriers for chemisorption of D_2 and CH_4 are quite similar, but those for CO and N_2 are significantly larger for Si_{25}^+ than for Al_{25}^+. This may indicate that Si_{25}^+ is considerably less effective as a π donor than Al_{25}^+, but the clusters are roughly equivalent as σ donors.

(37) Richtsmeier, S. C.; Parks, E. K.; Liu, K.; Pobo, L. G.; Riley, S. J. *J. Chem. Phys.* **1985**, *82*, 3659. Morse, M. D.; Geusic, M. E.; Heath, J. R.; Smalley, R. E. *J. Chem. Phys.* **1985**, *83*, 2293.
(38) Parks, E. K.; Weiller, B. H.; Bechthold, P. S.; Hoffman, W. F.; Nieman, G. C.; Pobo, L. G.; Riley, S. J. *J. Chem. Phys.* **1988**, *88*, 1622.
(39) Elkind, J. L.; Weiss, F. D.; Alford, J. M.; Laaksonen, R. T.; Smalley, R. E. *J. Chem. Phys.* **1988**, *88*, 5215.

Summary and Conclusions

In this paper we have presented the results of a detailed study of the reactions of Si_{25}^+ with a range of simple molecules. Many of the reactions studied show substantial activation barriers and so they can only be studied using methods, such as the ion beam technique, where a wide range of collision energies are accessible. Activation barriers for chemisorption of D_2, CH_4, O_2, C_2H_4, CO, and N_2 on Si_{25}^+ were derived from the experimental data. In many cases chemical reactions, resulting in cluster fragmentation, followed chemisorption. These chemical reactions often result in fission of the cluster, similar to the dissociation processes recently observed for the bare clusters. The data for the reactions of Si_{25}^+ were compared with our recently published results for Al_{25}^+. There are obvious similarities between the reactions of Al_{25}^+ and Si_{25}^+, despite the large differences expected in the bonding of these clusters. The activation barriers show the same qualitative trends, but there are also significant differences. Al_{25}^+ does not undergo the fission processes observed with Si_{25}^+. The activation barriers for chemisorption on both Al_{25}^+ and Si_{25}^+ show a qualitative correlation with the cluster HOMO $\rightarrow$ molecule LUMO promotion energy, suggesting that charge-transfer stabilization of the transition state is an important factor in determining the size of the activation barriers for chemisorption on atomic clusters. The electronic structure of the metal cluster and the strength of the bonds being broken and formed are probably also important.

Acknowledgment. We are grateful for a number of helpful comments by the reviewers, and by M. L. Mandich.

Isomeric Characterization of Gaseous Ions. Minimizing $C_4H_8^{\bullet+}$ Rearrangement by Dissociating the Corresponding Neutrals

Rong Feng, Chrysostomos Wesdemiotis, Mei-Yi Zhang, Mauro Marchetti, and Fred W. McLafferty*

Contribution from the Department of Chemistry, Baker Laboratory, Cornell University, Ithaca, New York 14853-1301. *Received August 22, 1988*

Abstract: With use of neutralization–reionization (NR) mass spectrometry, five gaseous $C_4H_8^{\bullet+}$ isomers can be structurally characterized by neutralization with sodium to produce excited C_4H_8 molecules whose dissociation products are reionized to both negative and positive ions. Such NR mass spectra are less characteristic when produced by Cs neutralization, which forms more highly excited C_4H_8, or by Hg neutralization followed by dissociation of C_4H_8 using multiple collisions; on average each collision adds ~1.7 eV to the molecule, so that isomerization may occur between collisions. The Na NR spectra show that $C_4H_8^{\bullet+}$ ions from all butyl acetate isomers have the expected structure except that 2-$C_4H_8^{\bullet+}$ is formed from *n*-butyl acetate. 2-$C_4H_8^{\bullet+}$ and methylcyclopropane$^{\bullet+}$ appear to be the major products from methylcyclopentane$^{\bullet+}$. 1-Butanol$^{\bullet+}$ and cyclohexane$^{\bullet+}$ predominantly form cyclobutane$^{\bullet+}$, while β- and γ-valerolactone$^{\bullet+}$ give 1-$C_4H_8^{\bullet+}$ and methylcyclopropane$^{\bullet+}$, respectively, as major products.

Recent impressive advances in the chemistry of gaseous ions, and the applications of this chemistry to synthesis and analysis, have depended heavily on techniques for ion structural characterization.[1,2] For example, valuable new information on simple ions in plasmas has come from laser spectroscopy.[3] However, a long-term problem for the identification of isomeric cations, especially those of hydrocarbons, has been their low isomerization barriers,[4] both low in absolute terms (13–30 kcal mol^{-1} for $C_4H_8^{\bullet+}$ isomers, Table I) and low relative to the isomerization barriers for the corresponding neutrals (64–73 kcal mol^{-1} for C_4H_8 iso-

(1) (a) Zwinselman, J. J.; Nibbering, N. M. M.; Ciommer, B.; Schwarz, H. In *Tandem Mass Spectrometry*; McLafferty, F. W., Ed.; Wiley: New York, 1983; pp 67–104. (b) Bowers, M. T., Ed. *Gas Phase Ion Chemistry*; Academic Press: New York, 1984.
(2) McLafferty, F. W.; Turecek, F. *Interpretation of Mass Spectra*, 4th ed.; University Science Books: Mill Valley, CA, 1989.
(3) Saykally, R. J. *Science* **1988**, *239*, 157–161.
(4) (a) Meisels, G. C.; Park, J. Y.; Giessner, B. G. *J. Am. Chem. Soc.* **1970**, *92*, 254–258. (b) Smith, G. A; Williams, D. H. *J. Chem. Soc. B* **1970**, 1529–1532. (c) Bowen, R. D.; Williams, D. H. *Org. Mass Spectrom.* **1977**, *12*, 453–460. (d) Holmes, J. L.; Weese, G. M.; Blair, A. S.; Terlouw, J. K. *Ibid.* **1977**, *12*, 424–431. (e) Baer, T.; Smith, D.; Tsai, B. P.; Wer, A. S. *Adv. Mass Spectrom.* **1978**, *7A*, 56–62. (f) Hsieh, T.; Gilman, J. P.; Weiss, M. J.; Meisels, G. G. *J. Phys. Chem.* **1981**, *85*, 2722–2725.

0002-7863/89/1511-1986$01.50/0